Smart Structures and Systems, *Vol. 28, No. 3 (2021) 363-373*
https://doi.org/10.12989/sss.2021.28.3.363

Elimination of moving vehicles effects on modal identification of beam type bridges

Wen-Yu He [1,2a], Xu-Cong Ding [1,2b], Wei-Xin Ren*[3] and Yue-Ling Jing [1,2c]

[1] *Department of Civil Engineering, Hefei University of Technology, Hefei, Anhui Province, 230009, China*
[2] *Anhui Engineering Laboratory for Infrastructural Safety Inspection and Monitoring, Hefei, Anhui Province, 230009, China*
[3] *College of Civil and Transportation Engineering, Shenzhen University, Shenzhen, Guangdong Province, 518061, China*

(*Received September 21, 2020, Revised January 11, 2021, Accepted March 19, 2021*)

Abstract. The modal parameters identified under operation conditions are normally employed for bridge damage detection. However, the moving vehicles are usually deemed as part of the operation conditions without considering their mass property. Thus, the identified modal parameters belong to the vehicle-bridge system rather than the bridge itself, which would affect the effectiveness of subsequent damage detection. In this paper, the effects of moving vehicles on the identified frequencies and mode shapes under operation conditions are investigated via finite element model. The necessary of considering the moving vehicle effects is demonstrated by comparing the modal parameters variations induced by the moving vehicle and bridge damage. Then the empirical formulas to eliminate the moving vehicle effects considering the vehicle mass, velocity, bridge span and relative position are established by using the orthogonal test and least square method. Finally, examples are conducted to verify of the effectiveness of the proposed empirical formulas.

Keywords: modal parameter; moving vehicle; operation condition; stochastic subspace identification

1. Introduction

The modal parameters (natural frequencies and mode shapes) are important indicators in reelecting bridge property, which are normally used for finite element model (FEM) updating (Haidarpour and Tee 2020), damage detection (Ren and Roeck 2002, Fan and Qiao 2011), and condition assessment (Carden and Fanning 2004). Thus, modal identification is a crucial task in the field of bridge health monitoring and inspection (Li *et al*. 2010, Yang *et al*. 2020, Chen *et al*. 2020). As no need for valuable equipment to excite the bridge and arduous in-put measurement, the ambient excitation based methods such as Stochastic Subspace Method (SSI) are widely used (Peeters and Roeck 1999, Shimpi *et al*. 2019). As it is difficult to measure the excitation for real bridges, the moving vehicles are usually deemed as part of the operation conditions without considering their mass property though the general condition for applying SSI is stochastic excitation. However, the moving vehicle and bridge forms a moving vehicle-bridge system, and the identified modal parameters belong to the system instead of the bridge, which would bring disturb into the following damage detection process.

The vehicle effects on the measured frequencies of a bridge have been investigated systematically. Ladislav and Thomas (1996) calculated the frequencies of the vehicle-bridge system by assuming the vehicle as distributed mass, and deduced the computational formula to obtain the bridge natural frequencies from the vehicle-bridge system frequencies. Li and Su (Li *et al*. 2003) solved the eigenvalues of the motion equation of vehicle-bridge system to obtain the system frequencies, and provided the estimation formula for bridge natural frequency. Ren *et al*. (2011) studied the effects of vehicle parameters on the bridge frequencies, and the vehicle stiffness and vehicle mass were found to be the most significant factors. Daniel and Obrien (2013) discussed the influences of different vehicle-bridge frequency and mass ratio on the system frequencies, and the results indicated that for central vehicle-bridge frequency and mass ratio, the system frequencies may higher than bridge frequencies. Similar results were obtained by Daniel and Anders (2017) via FEM. Using the spring-mass model to simulate the vehicle-bridge system, Yang *et al*. (2013) investigated the system frequency change rule and presented the corresponding closed-form solution. Chang *et al*. (2014) pointed out the frequencies of the bridge and the vehicle-bridge systems were different, and established the analytical solution of the vehicle-bridge system with the vehicle parked at different locations. Liu *et al*. (2018) examined the influence law of different parameters of spring-mass system on the modal characteristics of Timoshenko beam via experiment and FEM. Actually, the dynamic characters of a system are not only determined by the stiffness and mass, but also their distribution. Taking advantages of this fact, He and Ren (2018) proposed a damage detection method for bridge structures based on a parked vehicle induced frequencies

*Corresponding author, Ph.D., Professor,
E-mail: renwx@szu.edu.cn
[a] Ph.D., Professor, E-mail: wyhe@hfut.edu.cn
[b] Master, E-mail: 2514913253@qq.com
[c] Ph.D., E-mail: jing@hfut.edu.cn

http://www.techno-press.org/?journal=sss&subpage=7
ISSN: 1738-1584 (Print), 1738-1991 (Online)

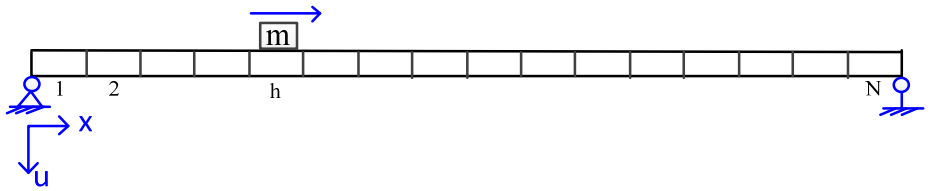

Fig. 1 FEM of simply supported beam subjected to a moving vehicle (mass)

variation. Further He *et al*. (2018) established the relationship between a parked vehicle induced frequencies changes and the mode shapes, and put forward a corresponding mode shape identification method.

In addition to the above-mentioned theoretical, numerical and experimental analysis, filed tests were also conducted to investigate the vehicle effects on the natural frequencies of vehicle-bridge system in real environment. Askegaard and Mossing (1988) monitored the frequency of a three-span concrete bridge for three years, and the results showed that the system frequency was significantly different from bridge frequency when there were vehicles on the bridge. Farra *et al*. (1997) conducted long-term health monitoring on a bridge, and the frequency of the vehicle-bridge system decreased by 6.4% when only the influence of the dead weight of the vehicles on the bridge was considered. Kim *et al*. (2003) tested a real bridge in operation and discussed the influence of vehicle mass on the system frequency. When the vehicle was parked on the bridge, the frequency of the system decreased by 5.4% compared with the natural frequency of the bridge. Spiridonakos and Fassois (2009) measured natural frequencies of vehicle-bridge systems in field, and significant changes were observed when the mass ratio of vehicle to bridge was relatively large. Feng *et al*. (2017) carried out field tests on the bridge in operation, and used time-frequency tools to analyze the frequency variation law of the bridge when the test truck was running on the bridge. The results showed that the frequency changed with the vehicle weight and vehicle position.

Though adequate attention has been paid to the vehicle effects on the natural frequencies, in-depth study on the vehicle effects on mode shapes still remains to be done. Daniel *et al*. (2017) conducted field experiments on two real bridges and concluded that the bridge frequencies and modes shapes changed when the vehicle was in different positions. Besides, most studies are focused on the parked vehicle effects rather than moving vehicle effect, which is different from the actual situation. Without considering on the mass property of moving vehicles, the identified modal parameters belong to the vehicle-bridge system. The differences of modal parameters between the bridge and vehicle-bridge system would raise a challenging task in the following damage detection in which modal parameters of the bridge are required. This paper aims to investigate the moving vehicles effects on the identified modal parameters of beam type bridges under operation conditions, and provide empirical formulas to estimate the real natural frequencies and mode shapes from the measured ones. Firstly, FEM simulation is conducted to study the frequencies and mode shapes obtained by SSI method. Then the empirical formulas to eliminate the moving vehicle effects are established by using the orthogonal test and least square method, and verified by numerical and experimental examples.

2. Motion equation of the vehicle-bridge system

In view of the complexity of actual bridge and load, FEM is normally employed to calculate the dynamic response of vehicle-bridge system. Taking a simply supported beam as an example (Fig. 1), the basic procedure of dynamic response calculation is briefly described in this section. For convenience of implementation, the vehicle is simplified as a moving mass without considering its stiffness and damping, and the bridge is simulated via plane Euler beam element.

As shown in Fig. 1, the simply supported beam is divided into N elements with equal length. The motion equation of the beam is

$$M_b\ddot{u} + C_b\dot{u} + K_b u = f(t) \tag{1}$$

in which M_b,C_b and K_b are the mass matrix, damping matrix and stiffness matrix of the beam, respectively. Rayleigh damping is adopted, thus the damping matrix can be calculated as $C_b = a_1 M_b + a_2 K_b$ (a_1 and a_2 are constant factors). $\ddot{u}$, $\dot{u}$ and u are the acceleration, velocity and displacement response, respectively. $f(t)$ is external load vectors, including vehicle and other environmental excitations.

When the beam is simulated via FEM, the displacement field in each element is approximated by shape functions. As for the Euler beam, cubic polynomial is used as the shape function (Lu and Liu 2011), specific as

$$B_h = \begin{Bmatrix} 1 - 3\left(\dfrac{x-(h-1)l}{l}\right)^2 + 2\left(\dfrac{x-(h-1)l}{l}\right)^3 \\ (x-(h-1)l)\left(\left(\dfrac{x-(h-1)l}{l}\right) - 1\right)^2 \\ 3\left(\dfrac{x-(h-1)l}{l}\right)^2 - 2\left(\dfrac{x-(h-1)l}{l}\right)^3 \\ (x-(h-1)l)\left(\dfrac{x-(h-1)l}{l}\right)^2 - \dfrac{(x-(h-1)l)^2}{l} \end{Bmatrix} \tag{2}$$

in which h is the elemental number, $(h-1)l \le x = vt \le hl$, x is the distance between the vehicle location and the origin of the coordinate, v is the vehicle velocity, and l is the elemental length.

Considering the mass property, the vehicle induced

additional mass matrix can be expressed as

$$\bar{M} = mB_h B_h^T \tag{3}$$

Then this additional mass matrix is superimposed on the corresponding position of the original mass matrix of the beam to form the total mass matrix (M_s) of the vehicle-beam system.

$$M_s = M_b + \begin{bmatrix} 0 & \cdots & 0 & \cdots & 0 \\ \vdots & \ddots & \vdots & \iddots & \vdots \\ 0 & \cdots & \bar{M}_{4\times4} & \cdots & 0 \\ \vdots & \iddots & \vdots & \ddots & \vdots \\ 0 & \cdots & 0 & \cdots & 0 \end{bmatrix}_{n\times n} \tag{4}$$

Thus, the motion equation of vehicle-beam system is

$$M_s\ddot{u} + C_b\dot{u} + K_b u = f(t) \tag{5}$$

The dynamic response of the system can be obtained via solving Eq. (5) step by step. Since the matrixes K and M are time-varying, the corresponding natural frequencies and mode shapes would also be time-varying.

Special signal processing tools are normally required to perform on the dynamic responses collected by sensors for natural frequencies and mode shapes. In this study, SSI widely used for bridges under operation conditions (Peeters and Roeck 1999, Li *et al*. 2016) is employed for modal identification.

3. Moving vehicle effects on the identified modal parameters

Taking a simply supported beam as example, this section investigates the effects of moving vehicle on the identified modal parameters, and demonstrates the necessary of considering the moving vehicle effects by comparing the changes of frequencies and mode shapes induced by the moving vehicle and local damage.

The main parameters of the beam are: the beam length is 30 m, the elasticity modulus is 27.5 Gpa, the constant mass density is 1000 kg/m, and the inertia moment is 0.175 m^4. The weight and velocity of the vehicle are 1000 kg and 1 m/s, respectively. The beam contains 30 Euler beam elements with equal length and 31 nodes in FEM simulation. The damages are simulated by elemental bending stiffness reduction. The 7th, 19th, and 25th elements are assumed to be damaged elements with the severities of 25%. Gaussian white noise is applied at all degree-of-freedoms to simulate the operation conditions. Four cases are considered in this simulation, specific as: (1) Case 1: undamaged beam; (2) Case 2: beam with local damage; (3) Case 3: undamaged beam subjected to a moving vehicle; (4) Case 4: beam with local damage subjected to a moving vehicle. The dynamic responses are then calculated via the FEM. Then responses of the 4th, 10th, 16th, 22th, and 28th nodes are employed to identify the natural frequencies and mode shapes of the four cases via SSI. It should be noted that the mode shapes will be normalized according to the maximum value.

Table 1 Frequency variations of the simple supported beam (Hz)

Frequency varition	First mode	Second mode	Third mode
FV2-1	-0.07	-0.23	-1.07
FV3-1	-0.05	-0.11	-0.30
FV4-1	-0.11	-0.33	-1.81

Table 2 Relative variations of the 3rd mode shape of the simple supported beam (%)

Relative variation	Node 4	Node 10	Node 16	Node 22	Node 28
RVMS2-1	-3.93	-4.21	0.00	-2.23	-1.44
RVMS3-1	0.37	-1.53	0.00	-0.03	-0.68
RVMS4-1	-3.98	-5.32	0.00	-2.54	2.48

Since Case 1 involves no damage and no vehicle, the corresponding modal parameters belong to the beam itself. To better illustrate the influences of different factors (damage, moving vehicle, damage and moving vehicle together), the variations between Case 2, Case 3, Case 4, and Case 1 are compared in Table 1. It can be seen that the damage induced frequency variations for the first three modes are -0.07 Hz, -0.23 Hz and -1.07 Hz, respectively; the moving vehicle induced frequency variations for the first three modes are -0.05 Hz, -0.11 Hz and -0.3 Hz, respectively; the damage and moving vehicle induced frequency variations for the first three modes are -0.11 Hz, -0.33 Hz and -1.81 Hz, respectively. Obviously, the damage and moving vehicle all results in frequency variations. Besides, the frequency variation ranges larger when the beam subjected to both damage and moving vehicle at the same time.

As the variation of the third mode is larger than the others, here only the relative variations of the third mode shape at the 4th, 10th, 16th, 22th, and 28th nodes are compared in Table 2. Similarly, to the frequency, both local damage and moving vehicle lead to variations in the identified mode shapes. Without considering the moving vehicle effects, the frequency and mode shape variation would be misjudged as induced by damages, which would bring disturb into the following damage detection process. Therefor it is essential to eliminate the moving vehicles effects on modal identification.

4. Elimination of moving vehicle effects

As illustrated in Section 3, it is essential to eliminate the moving vehicles effects on modal identification of bridges under operation conditions. This section aims to establish the empirical formulas of frequency and mode shape which can eliminate the effects of moving vehicles.

4.1 Elimination of moving vehicle effects on frequency

In actual modal test, the frequencies are determined via

the dynamic response collected by sensors. It should be noted that the identified frequency ($\omega(V)$) normally includes the moving vehicle effects when the bridge is subjected to moving vehicles. The frequency of the bridge itself (ω) can be obtained when the moving vehicle effects is eliminated.

For convenience, frequency variation coefficient is defined as

$$FV^i = \frac{\omega}{\omega^i(V)} \tag{6}$$

in which FV^i denotes the frequency variation coefficient obtained by the i^{th} test, ω denotes the frequency of the bridge, and $\omega^i(V)$ denotes the identified frequency of the vehicle-bridge system in the i^{th} test.

According to Eq. (6), an empirical formula reflecting the coefficient of frequency variation and moving vehicle effects can be established, which can be used to eliminate the moving vehicle effects for the frequency belong to the bridge

$$\omega = \overline{FV} \times \omega^i(V) \tag{7}$$

in which $\overline{FV}$ denotes the empirical formula for frequency variation coefficient.

Table 3 Design of the orthogonal test for frequency

Level	Vehicle mass (kg)	Vehicle velocity (m/s)	Bridge span (m)
Level 1	1000	1	16
Level 2	2000	2	24
Level 3	3000	4	32
Level 4	4000	8	40
Level 5	5000	16	48

In this section, the vehicle mass, vehicle velocity and bridge span are considered as the most influential factors. And the first frequency of a simply supported beam is taken an example to establish the empirical formula. Firstly, the influence law between the frequency variation coefficient and each single factor is obtained by using orthogonal experimental design and statistical analysis. Then the functional relation between the frequency variation coefficient and each single factor is assumed according to the influence law. Finally, the empirical formula is synthesized by all factors via the least square method.

In addition to the span, the parameters of the simply supported beam are the same as in Section 3. The specific values of the three factors are shown in Table 3, and five levels are considered for each factor. The orthogonal experiment $L_{25}(5^4)$ including 25 tests is arranged accordingly. SSI is employed to identify the first frequency of the bridge without moving vehicle (ω) and the first frequencies of the 25 tests with a vehicle running on the beam. Then the frequency variation coefficients are calculated via Eq. (6). Finally, the influence law between the FVs and three factors are obtained by using statistical analysis of 25 tests and shown in Fig. 2, respectively. Judging by Fig. 2, the FV is positively associated with change in vehicle mass and vehicle velocity, and inversely associated with bridge span.

According to the influence law of a single factor, the relationships can be assumed as follows:

(1) As FV increases gradually with the vehicle mass (Fig. 2(a)), assuming that $FV = \alpha_1 x_1^{\alpha_2} + \alpha_3$ (α_1, α_2 and α_3 denote constants to be determined, and x_1 denotes the vehicle mass).
(2) As FV increases gradually with the vehicle velocity

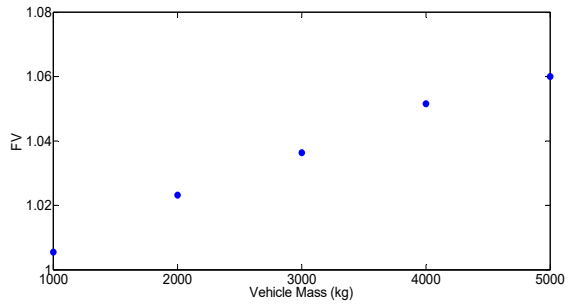

(a) Vehicle mass effects

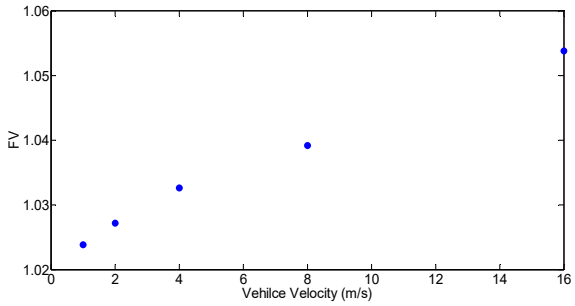

(b) Vehicle velocity effects

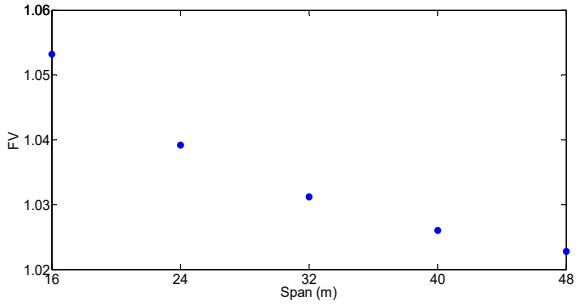

(c) Span effects

Fig. 2 Moving vehicle induced frequency variation

Table 4 Fitting coefficients for frequency

Coefficient	α_1	α_2	α_3	α_4	α_5	α_6	α_7	α_8	α_9
Fitting value	0.0658	0.6632	-0.1852	0.0233	0.8759	0.0814	0.3821	1.1228	1.0118

(Fig. 2(b)), assuming that $FV = \alpha_4 x_2^{\alpha_5} + \alpha_6$ (α_4, α_5 andα_6 denote constants to be determined, and x_2 denotes the vehicle velocity).

(3) As FV decreases gradually with the vehicle span (Fig. 2(c)), assuming that $FV = \alpha_7 / x_3^{\alpha_8}$ (α_7 and α_8 denote constants to be determined, and x_3 denotes the bridge span).

Thus, the empirical formula considering the three influencing factors together can be assumed as

$$FV = (\alpha_1 x_1^{\alpha_2} + \alpha_3)(\alpha_4 x_2^{\alpha_5} + \alpha_6)(\alpha_7 / x_3^{\alpha_8}) + \alpha_9 \quad (8)$$

The fitting coefficients ($\alpha_1, \alpha_2 \cdots \alpha_9$) are then estimated by the least square method as listed in Table 4. With these fitting coefficients, the empirical formula for estimating the frequency variation can be calculated via Eq. (8). Then the frequency after eliminating the moving vehicles effects can be obtained via Eq. (7). Numerical example will be conducted to verify the effectiveness of the proposed empirical formula. The parameters of the numerical beam are still the same as those in Section 3.

Firstly, the empirical formula for eliminating the effects of different vehicle mass is verified. The bridge span and vehicle velocity are set to be 40 m and 4 m/s, receptively. Different vehicle masses are assumed in simulation and the frequencies are identified accordingly. The frequency without moving vehicle effects, frequency containing moving vehicle effects and the frequency processed by the empirical formula are compared in Fig. 3. The specific values of frequency variation with different vehicle mass are shown in Table 5. It can be seen that after eliminating the moving vehicles effects through empirical formula, the frequency variation with different vehicle masses decreases significantly, and the processed result is very close to the frequency without moving vehicle effect. For example, the frequency variation is changed from -0.064 Hz to -0.007 Hz when the vehicle mass is 4000 kg. Following the same procedure, the effectiveness of the empirical formulas for eliminating the effects of different vehicle velocity and bridge span is verified. The corresponding results are shown in Tables 6 and 7, respectively. Similarly, moving vehicles effects are eliminated effectively through the empirical

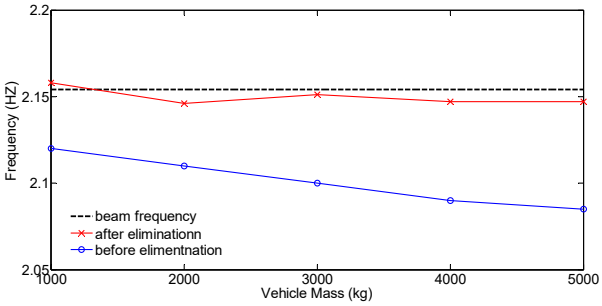

Fig. 3 Frequency variation processed by the empirical formula with different vehicle mass

Table 5 Frequency variation with different vehicle mass processed by the empirical formula (Hz)

Frequency	1000 kg	2000 kg	3000 kg	4000 kg	5000 kg
BF	2.154	2.154	2.154	2.154	2.154
IF	2.121	2.110	2.100	2.090	2.085
DBFIF	-0.033	-0.044	-0.054	-0.064	-0.069
IFAE	2.159	2.155	2.151	2.147	2.147
DBFIFAE	0.005	0.001	-0.003	-0.007	-0.007

*Note: BF denotes the bridge frequency; IF denotes the identified frequency; DBFIF denotes the difference between the BF and IF; IFAE denotes the IF after eliminating moving vehicle effects; DBFIFAE denotes the difference between the BF and IFAE

Table 6 Frequency variation with different vehicle velocity processed by the empirical formula (Hz)

Frequency	1 m/s	4 m/s	8 m/s	12 m/s	16 m/s
BF	2.154	2.154	2.154	2.154	2.154
IF	2.121	2.110	2.100	2.090	2.085
DBFIF	-0.033	-0.044	-0.054	-0.064	-0.069
IFAE	2.159	2.155	2.151	2.147	2.147
DBFIFAE	0.005	0.001	-0.003	-0.007	-0.007

*Note: The meanings of BF, IF, DBFIF, IFAE and DBFIFAE are the same as in Table 5

Table 7 Frequency variation with different span processed by the empirical formula (Hz)

Frequency	16 m	24 m	32 m	40 m	48 m
BF	13.461	5.983	3.365	2.154	1.496
IF	13.120	5.814	3.300	2.118	1.475
DBFIF	-0.341	-0.169	-0.065	-0.036	-0.021
IFAE	13.552	5.961	3.370	2.159	1.501
DBFIFAE	0.091	-0.022	0.005	0.005	0.005

*Note: The meanings of BF, IF, DBFIF, IFAE and DBFIFAE are the same as in Table 5

Table 8 Cases for frequency empirical formula verification

Case	Vehicle mass (kg)	Vehicle velocity (m/s)	Bridge span (m)
Case 5	2000	2	24
Case 6	3000	4	32
Case 7	4000	8	40

Table 9 Frequency verification results of the empirical formula (Hz)

Case	Case 5	Case 6	Case 7
BF	5.983	3.365	2.154
IF	5.814	3.232	2.081
DBFIF	-0.169	-0.133	-0.073
IFAE	5.961	3.323	2.151
DBFIFAE	-0.022	-0.042	-0.003

*Note: The meanings of BF, IF, DBFIF, IFAE and DBFIFAE are the same as in Table 5

formula.

Finally, the applicability of the proposed empirical formula when the comprehensive influences of three factors are considered is examined via three cases involving different vehicle mass, vehicle velocity and span (Table 8). Noted that the three cases are not used in establish the empirical formula. The verification results of empirical formula for frequency are shown in Table 9. Though significant variations can be found in the initial results (-0.169 Hz, -0.133 Hz, and -0.073 Hz), the frequencies disposed by the empirical formula agree well with the frequencies of the beam itself, which indicates that the proposed empirical formula is effective in eliminating the moving vehicles effects.

4.2 Elimination of moving vehicle effects on mode shape

Unlike frequency, empirical formulas for eliminating the moving vehicle effects on mode shape are established for the left half span and right half span of the simply supported beam respectively. The first order mode shape identified with and without a moving vehicle is deemed as ϕ^V and ϕ, respectively. The difference between mode shapes (normalized according to the maximum value) with and without moving vehicle effects is defined as mode shape variation (MSV). For the right and left half span, the MSV can be written as

$$MSV_L = \phi_L - \phi_L^V \tag{9a}$$

$$MSV_R = \phi_R - \phi_R^V \tag{9b}$$

in which L and R denote the right hale span and left half span, respectively.

Similar to frequency, orthogonal experimental design is adopted to establish the relationship between the MSV and influencing factors. In particular, the position should be considered in the design of orthogonal test as the values of mode shape at different positions are not the same. The relative position is defined as the ratio of coordinate value to the bridge length (Fig. 1). The left half span and the right half span are considered respectively. The final orthogonal experimental design for mode shape is shown in Table 10.

The orthogonal experiments $L_{25}(5^4)$ including 25 tests are arranged for the left half span and the right half span, respectively. The SSI is employed to identify the first mode shape of the beam with and without moving vehicle effects and the MSV of left half span and right half span are obtained accordingly. The relationship between the MSV and the four factors are shown in Figs. 4 and 5. The absolute value of MSV is found to be positively associated with change in vehicle mass and vehicle velocity, and inversely associated with bridge span. Besides, the absolute value of MSV increases first and then decreases with the increasing of the relative position.

Taking the left half span as an example, the following relationships are assumed according to the influence law of single factor for the mode shape:

(1) As the absolute value of MSV increases gradually with the vehicle mass, and it is equal to zero when the vehicle mass is zero, assuming $MSV = \lambda_1 x_1^{\lambda_2}$ (λ_1 and λ_2 denote constants to be determined, and x_1 denotes the vehicle mass).

Table 10 Design of the orthogonal test for mode shape

Span	Level	Vehicle mass (kg)	Bridge span (m)	Vehicle velocity (m/s)	Relative position
Left half span	Level 1	1000	16	1	1/12
	Level 2	2000	24	2	2/12
	Level 3	3000	32	4	3/12
	Level 4	4000	40	8	4/12
	Level 5	5000	48	16	5/12
Right half span	Level 1	1000	16	1	7/12
	Level 2	2000	24	2	8/12
	Level 3	3000	32	4	9/12
	Level 4	4000	40	8	10/12
	Level 5	5000	48	16	11/12

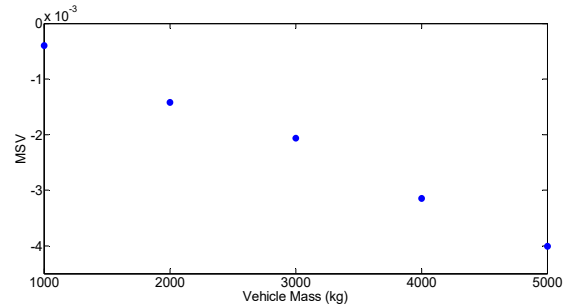

(a) Vehicle mass effects

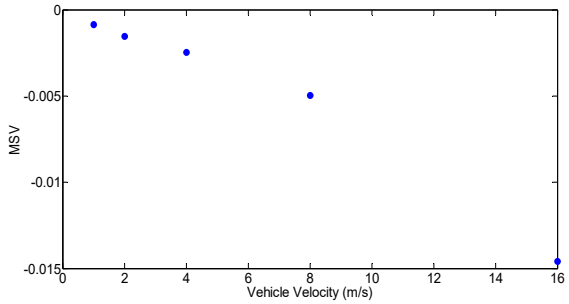

(b) Vehicle velocity effects

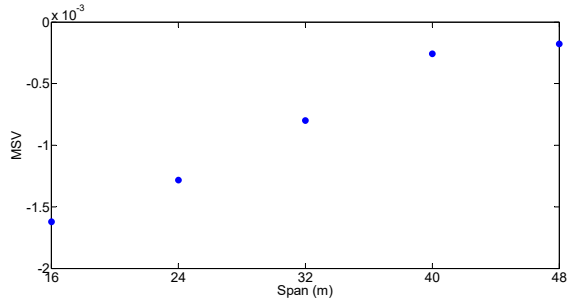

(c) Span effects

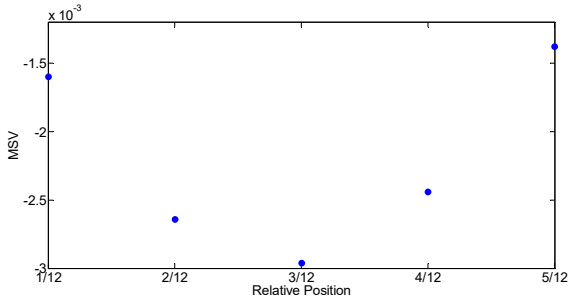

(d) (d) Relative position effects

Fig. 4 Moving vehicle induced mode shape variation of the left half span

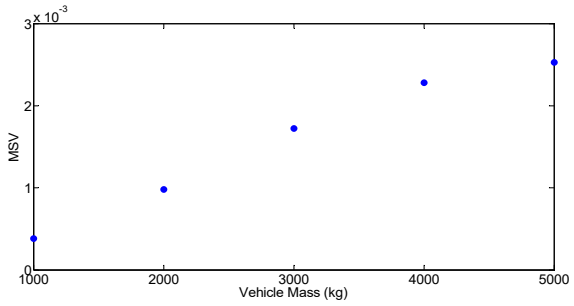

(a) Vehicle mass effects

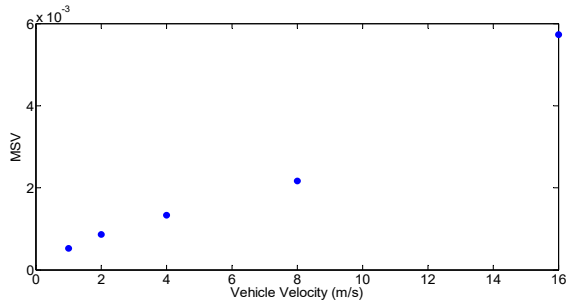

(b) Vehicle velocity effects

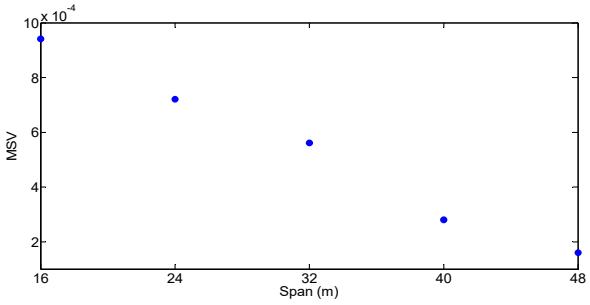

(c) Span effects

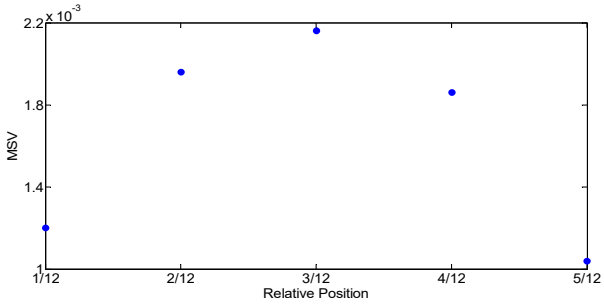

(d) Relative position effects

Fig. 5 Moving vehicle induced mode shape variation of the right half span

(1) As the absolute value of MSV increases gradually with the vehicle velocity, assuming $MSV = \lambda_3 x_2^{\lambda_4} + \lambda_5$ (λ_3, λ_4 and λ_5 denote constants to be determined, and $x_2$denotes the vehicle velocity).

(2) As the absolute value of MSV decreases gradually with the vehicle span, assuming $MSV = \lambda_6 / x_3^{\lambda_7}$ (λ_6 and λ_7 denote constants to be determined, and x_3 denotes the bridge span).

(3) As the relationship of the absolute value of MSV and relative position shows the parabolic trend, assuming $MSV = \lambda_8 x_4^2 + \lambda_9 x_4 + \lambda_{10}$ (λ_8, λ_9 and λ_{10} denote constants to be determined, and x_4 denotes the relative position)

Thus, the empirical formula considering the four influence factors for the left half span can be assumed as

Table 11 Fitting coefficients for mode shape

Left half span		Right half span	
λ_1	-5.50×10^{-6}	μ_1	4.2102
λ_2	0.9570	μ_2	0.6587
λ_3	0.5520	μ_3	1.8596
λ_4	1.5092	μ_4	1.0849
λ_5	0.2439	μ_5	0.8675
λ_6	2.9594	μ_6	4.62×10^{-6}
λ_7	1.0384	μ_7	0.8070
λ_8	0.4681	μ_8	0.3292
λ_9	0.4534	μ_9	0.4183
λ_{10}	0.7046	μ_{10}	0.5408
λ_{11}	4.69×10^{-5}	μ_{11}	-3.89×10^{-4}

$$MSV_L = \left(\lambda_1 x_1^{\lambda_2}\right)\left(\lambda_3 x_2^{\lambda_4} + \lambda_5\right)\left(\frac{\lambda_6}{x_3^{\lambda_7}}\right) \left(\lambda_8 x_4^2 + \lambda_9 x_4 + \lambda_{10}\right) + \lambda_{11} \tag{10}$$

in which $\lambda_1, \lambda_2 \cdots \lambda_{11}$ denote constants to be determined.

Similarly, the empirical formula for the right half span can be assumed as

$$MSV_R = \left(\mu_1 x_1^{\mu_2}\right)\left(\mu_3 x_2^{\mu_4} + \mu_5\right)\left(\frac{\mu_6}{x_3^{\mu_7}}\right) \left(\mu_8 x_4^2 + \mu_9 x_4 + \mu_{10}\right) + \mu_{11} \tag{11}$$

in which $\mu_1, \mu_2 \cdots \mu_{11}$ denote constants to be determined.

The fitting coefficients are then estimated by the least square method and show in Table 11. In the actual test, the identified mode shape containing moving vehicle effects (ϕ^{vi}) is divided into two parts, i.e., ϕ_L^V and ϕ_R^V. Then the $\Delta\phi_L$ and $\Delta\phi_R$can be obtained via empirical formulas (Eqs. (10) and (11)). Further Eqs. (9a) and (9b) are used to estimate the mode shape eliminating the moving vehicle effects (ϕ_L and ϕ_R). Finally, the whole mode shape without containing moving vehicle effects is synthesized accordingly.

The empirical formula considering the comprehensive influence of four factors is verified by using the Cases 5-6 as used in Section 4.2. The relative variations of the mode shape before and after eliminating moving vehicle effects are compared in Table 12. Significant reduction is found in the relative variations of the mode shape when the moving vehicles effects are eliminated via the empirical formula. The results of numerical examples clearly indicate that the proposed empirical formula can effectively eliminate the moving vehicles effects on mode shape identification results.

5. Experimental verification

Experimental models of vehicle and beam are made in the laboratory to identify the frequency and mode shape of beam with and without a moving vehicle and verify the empirical formula established in Section 4 in laboratory environment.

The experiment set up is show in Fig. 6. The aluminum beam is selected to serve as a simply supported beam model. The length and cross-section of the main beam is 3m and 124 mm × 24 mm, respectively. Two separated beams are placed as leading beam for initial acceleration, and trailing beam for deceleration. The weight of the car is determined by the number of weights placed on the car (Fig. 7). The car is dried by a motor and the velocity can be adjusted through the motor frequency modulator. Baffles are installed on both sides of the beam to prevent the car drops during movement. Eight sensors equally spaced are installed in the bottom of the beam to measure the acceleration responses for modal identification (Fig. 8). The sampling frequency is set to be 1000 Hz.

Five tests with different vehicle mass and vehicle velocity are conducted to verify the proposed empirical formula (Table 13). Firstly, the acceleration responses of the beam of different tests are collected by acceleration sensors. Typical beam acceleration responses are shown in Fig. 9. Then the frequencies and mode shapes are identified via SSI. Typical stability diagram is shown in Fig. 10.

Table 12 Relative variations of the mode shape (%)

Relative position	Case 5		Case 6		Case 7	
	Before elimination	After elimination	Before elimination	After elimination	Before elimination	After elimination
1/12	-0.10	0.02	-0.35	-0.01	-0.55	0.38
2/12	-0.18	0.05	-0.42	-0.06	-0.68	0.35
3/12	-0.20	0.06	-0.56	-0.17	-0.85	0.25
4/12	-0.17	0.02	-0.44	-0.03	-0.70	0.48
5/12	-0.11	0.05	-0.37	-0.07	-0.60	0.67
7/12	0.09	0.01	0.18	0.01	0.28	-0.09
8/12	0.15	0.06	0.29	0.10	0.34	-0.06
9/12	0.17	0.07	0.34	0.12	0.40	-0.04
10/12	0.15	0.04	0.26	0.03	0.38	-0.09
11/12	0.09	-0.03	0.20	-0.05	0.30	-0.21

(a) Experimental arrangement

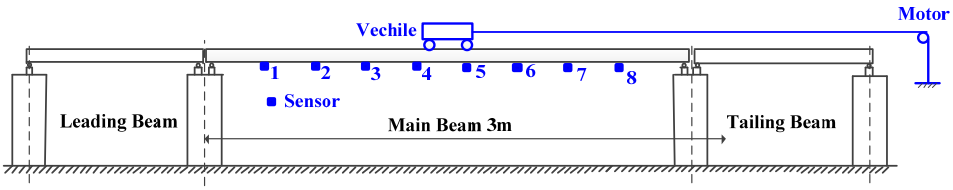

(b) Configuration of the beam

Fig. 6 Experimental arrangement and configuration of the beam

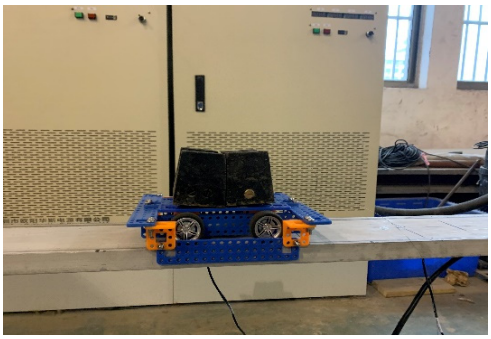

Fig. 7 Moving car

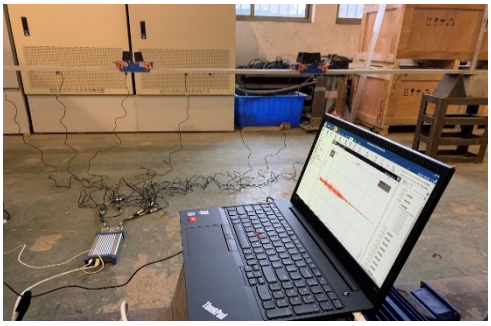

Fig. 8 Data acquisition system

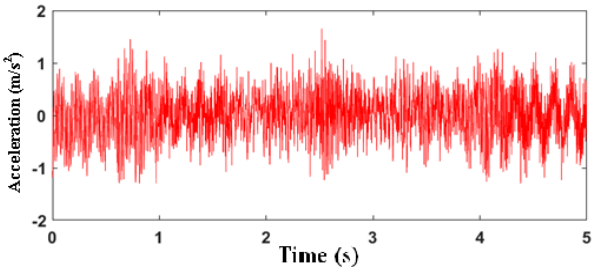

Fig. 9 Typical bridge acceleration response

Table 13 Vehicle parameters in the experiment

Test number	Test 1	Test 2	Test 3	Test 4	Test 5
Vehicle mass (kg)	No vehicle	4.3	4.3	6.3	6.3
Vehicle velocity(m/s)		0.6	1.2	0.6	1.2

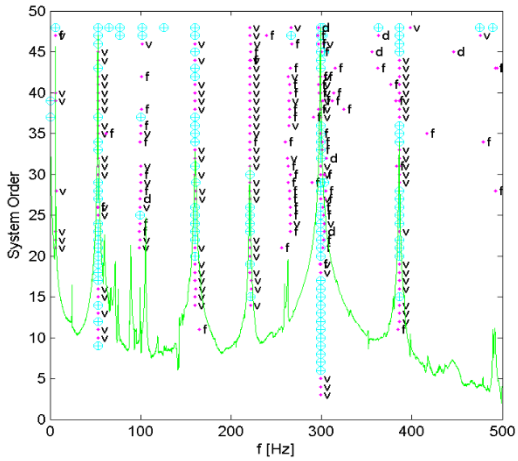

Fig. 10 Typical Stabilization plot

Table 14 Frequency results in the experiment (Hz)

Frequency	Test 2	Test 3	Test 4	Test 5
BF	6.000	6.000	6.000	6.000
IF	5.950	5.932	5.931	5.922
DBFIF	-0.050	-0.068	-0.069	-0.078
IFAE	6.020	6.001	6.003	5.995
DBFIFAE	0.020	0.000	0.003	-0.005

*Note: The meanings of BF, IF, DBFIF, IFAE and DBFIFAE are the same as in Table 5

Table 15 Model shape results in the experiment (%)

Relative position		1/9	2/9	3/9	4/9	5/9	6/9	7/9	8/9
Test 2	Before elimination	-0.06	-0.09	-0.06	-0.03	0.02	0.05	0.06	0.03
	After elimination	-0.03	-0.07	-0.03	-0.01	0.02	0.05	0.06	0.03
Test 3	Before elimination	-0.07	-0.09	-0.11	-0.04	0.03	0.08	0.11	0.07
	After elimination	0.03	0.04	0.06	0.01	0.01	0.06	0.08	0.04
Test 4	Before elimination	-0.09	-0.13	-0.07	-0.03	0.04	0.08	0.09	0.05
	After elimination	-0.06	-0.08	-0.04	0.00	0.04	0.08	0.09	0.03
Test 5	Before elimination	-0.08	-0.11	-0.08	-0.04	0.03	0.07	0.08	0.06
	After elimination	-0.03	-0.05	-0.02	0.03	0.01	0.04	0.04	0.01

The identified frequencies, bridge span, and vehicle parameters of Tests 2, 3, 4, and 5 are put into the empirical formulas, and the frequency variation coefficients are obtained accordingly. The frequency variations before and after eliminating moving vehicle effects are compared in Table 14. The maximal variations are 0.078 Hz and 0.020 Hz before and after performing the empirical formula. Compared to the identified frequencies, the frequencies processed by the empirical formula are closer to the frequencies without moving vehicle effect. The mode shape variations before and after eliminating the moving vehicle effects at the eight points are obtained according to Eqs. (9a) and (9b). Then, relative variations of first mode shapes at the eight points are compared in Table 15. It is observed that the relative variations are reduced after the elimination of moving vehicle effects. The experiment results indicate that the empirical formula is effective in eliminating the moving vehicle effects for modal identification in laboratory environment. It should be noted that the same empirical formulas are used in the experiment and in the simulation though the experimental beam is very different from the simulated one. Good results obtained in the experiment clearly indicate that the empirical formulas can be applied to more general case.

6. Conclusions

The moving vehicles are usually deemed as part of the operation conditions without considering their mass property in the modal identification of bridges. Thus, the identified modal parameters belong to the vehicle-bridge system rather than the bridge. It is essential to eliminate the moving vehicle effects for bridge health monitoring. In this paper, the effects of moving vehicle on the modal parameters obtained by SSI method under operation conditions were investigated via FEM. The results indicated that without considering the moving vehicle effects, the frequency and mode shape variation would be misjudged as induced by damages. The influence law between the modal variation and each single factor (vehicle mass, vehicle velocity, bridge span and relative position) was obtained by using orthogonal experimental design and statistical analysis. Then the functional relation between the modal variation and each single factor was assumed according to the influence law. Subsequently the empirical formula considering all factors was synthesized by using the least square method. Finally, numerical and experimental examples were conducted to verify of the effectiveness of the proposed empirical formulas. The results clearly manifested that the prosed empirical formula could eliminate the moving vehicles effects on frequency and mode shape identification results effectively. Though only the first mode of simply supported beam was investigated in this paper, empirical formulas for other modes or type of bridges can be obtained via similar procedures. Besides, further study on the effectiveness of the empirical formula for real bridge will be carried out through field test.

The stiffness and damping in a moving vehicle are not considered in this study. The damping of the moving vehicle will affect the amplitude of the dynamic response, but has limited influence on the identified frequencies and mode shapes. However, the influence of the vehicle stiffness on the dynamic response, identified frequencies and mode shapes is very complicated (Yang *et al*. 2013, Liu *et al*. 2018), and it is difficult to establish simple and practical formulas considering the vehicle stiffness effects. More systematic investigation on the vehicle stiffness effect would be conducted further.

Acknowledgments

The paper is supported by the National Natural Science Foundation of China (No. 51878234 and 51778204), Fundamental Research Funds for the Central Universities (No. JZ2019HGPA0101), Shenzhen Science and Technology Program (No. KQTD20180412181337494), and the Key Research and Development Project of Anhui Province (No. 1804a0802204).

References

Askegaard, V. and Mossing, P. (1988), "Long term observation of RC-bridge using changes in natural frequency", *Publication of Nordic Concrete Federation*.

Carden, E.P. and Fanning, P. (2004), "Vibration based condition monitoring: a review", *Struct. Helth Monitor.*, **3**(4), 355-377. https://doi.org/10.1177/1475921704047500

Chang, K.C., Kim, C.W. and Borjigin, S. (2014), "Variability in bridge frequency induced by a parked vehicle", *Smart Struct. Syst., Int. J.*, **13**(5), 755-773. https://doi.org/10.12989/sss.2014.13.5.755

Chen, G.W., Chen, X. and Omenzetter, P. (2020), "Modal

parameter identification of a multiple-span post-tensioned concrete bridge using hybrid vibration testing data", *Eng. Struct.*, **219**, 110953. https://doi.org/10.1016/j.engstruct.2020.110953

Daniel, C. and Anders, R. (2017), "Numerical evaluation of modal properties change of railway bridges during train passage", *Proc. Eng.*, **199**, 2931-2936. https://doi.org/10.1016/j.proeng.2017.09.345

Daniel, C. and Obrien, E.J. (2013), "The non-stationarity of apparent bridge natural frequencies during vehicle crossing events", *FME Trans.*, **41**(4), 279-284.

Daniel, C., David, H. and James, B. (2017), "Evolution of bridge frequencies and modes of vibration during truck passage", *Eng. Struct.*, **152,** 452-464. https://doi.org/10.1016/j.engstruct.2017.09.039

Fan, W. and Qiao, P.Z. (2011), "Vibration-based damage identification methods: a review and comparative study", *Struct. Health Monitor.*, **10**(1), 83-111. https://doi.org/10.1177/1475921710365419

Farrar, C., Doebling, S.W., Cornwell, P. and Bridge C. (1997), *Variability of modal parameters measured on the Alamosa Canyon Bridge*, (No. LA-UR-96-3953; CONF-970233-7). Los Alamos National Lab., NM, USA.

Feng, X., Gang, S.C., Hulsey, G.S. and Zatar, W. (2017), "Characterization of non-stationary properties of vehicle-bridge response for structural health monitoring", *Adv. Mech. Eng.*, **9**(5), 1-6. https://doi.org/10.1177/1687814017699141

Haidarpour, A. and Tee, K.F. (2020), "Finite element model updating for structural health monitoring", *Struct. Dura. Health Monitor.*, **14**(1), 1-17. https://doi.org/10.32604/sdhm.2020.08792

He, W.Y. and Ren, W.X. (2018), "Structural damage detection using a parked vehicle induced frequency variation", *Eng. Struct.*, **170**, 34-41. https://doi.org/10.1016/j.engstruct.2018.05.082

He, W.Y., Ren, W.X. and Zuo, X.H. (2018), "Mass normalized mode shape identification method for bridge structures using parking vehicle induced frequency change", *Struct. Control Hlth. Monit.* **25**, e2174.

Kim, C.Y., Jung, D.S., Kim, N.S., Kwon, S.D. and Feng, M.Q. (2003), "Effect of vehicle weight on natural frequencies of bridges measured from traffic-induced vibration", *Earthq. Eng. Eng. Vib.* **2**(1), 109-115. https://doi.org/10.1007/BF02857543

Ladislav, F. and Thomas, T. (1996), *Dynamics of Railway Bridges*.

Li, J.Z., Su, M.B. and Fan, L.C. (2003), "Natural frequency of railway girder bridges under vehicle loads", *J. Bridge Eng. ASCE*, **8**(4), 199-203. https://doi.org/10.1061/(ASCE)1084-0702(2003)8:4(199)

Li, H., Li, S., Ou, J. and Li, H. (2010), "Modal identification of bridges under varying environmental conditions: Temperature and wind effects", *Struct. Control Health Monitor.*, **17**(5), 495-512. https://doi.org/10.1002/stc.319

Li, D., Ren, W.X. Hu, Y.D. and Yang, D. (2016), "Operational modal analysis of structures by stochastic subspace identification with a delay index", *Struct. Eng. Mech., Int. J.*, **59**(1), 187-207. https://doi.org/10.12989/sem.2016.59.1.187

Liu, H., Wang, H., Tan, G. and Wang, W. (2018), "Effect of temperature and spring-mass systems on modal properties of Timoshenko concrete beam", *Struct. Eng. Mech., Int. J.*, **65**(4), 389-400. https://doi.org/10.12989/sem.2018.65.4.389

Lu, Z.R. and Liu, J.K. (2011), "Identification of both structural damages in bridge deck and vehicular parameters using measured dynamic responses", *Comput. Struct.*, **89**, 1397-1405. https://doi.org/10.1016/j.compstruc.2011.03.008

Peeters, B. and Roeck, G.D. (1999), "Reference-based stochastic subspace identification for output-only modal analysis", *Mech. Syst. Sig. Process.*, **13**(6), 855-878. https://doi.org/10.1006/mssp.1999.1249

Ren, W.X. and Roeck, G.D. (2002), "Structural damage identification using modal data. I: simulation verification", *J. Struct. Eng. ASCE*, **128**(1), 87-95. https://doi.org/10.1061/(ASCE)0733-9445(2002)128:1(87)

Ren, J.Y., Li, W.P. and Su, M.B. (2011), "Vertical load-carrying natural frequency of railway double-track pre-stressed concrete continuous bridge", *J. Rail. Eng. Soc.*, **255-260**(3), 797-800. https://doi.org/10.4028/www.scientific.net/AMR.255-260.797

Shimpi, V., Sivasubramanian, M.V.R. and Singh, S.B. (2019), "System identification of heritage structures through AVT and OMA: a review", *Struct. Dura. Health Monit.*, **13**(1), 1-40.

Spiridonakos, M.D. and Fassois, S.D. (2009), "Parametric identification of time-varying structure based on vector vibration response measurements", *Mech. Syst. Sig. Process.*, **23**(6), 2029-2048. https://doi.org/10.1016/j.ymssp.2008.11.004

Xiao, F., Chen, G.S., Hulsey, J.L. and Zatar, W. (2017), "Characterization of non-stationary properties of vehicle-bridge response for structural health monitoring", *Adv. Mech. Eng.*, **9**(5), 1-6. https://doi.org/10.1177/1687814017699141

Yang, Y.B., Cheng, M.C. and Chang, K.C. (2013), "Frequency variation in vehicle-bridge interaction systems", *Int. J. Struct. Stab. Dyn.*, **13**(2), 1-22. https://doi.org/10.1142/S0219455413500193

Yang, X.M., Yi, T.H., Qu, C.X., Li, H.N. and Liu, H. (2020), "Continuous tracking of bridge modal parameters based on subspace correlations", *Struct. Control Health Monitor.*, **27**(10), e2615. https://doi.org/10.1002/stc.2615

BS